



On Properties of Energetic Coronal Mass - Flare Events

M. Youssef

Physics Department, Faculty of Science, Helwan University, Ain Helwan, Egypt

ABSTRACT

In the present paper, the properties of more energetic coronal mass ejections (ECMEs) (kinetic energy $\geq 1E + 30$ ergs) observed between the years from 1996 to 2006 were studied. Through this period and under certain time-based and spatial conditions 253 Flare-ECMEs were selected. These 253 energetic CME-Flare events separated into two groups according to their time of detection, Before Flare-ECME events and After Flare-ECME event. This study indicates that the mean CME width for both before and after Flare-ECMEs are 90 and 100 degrees, respectively. Also, it was found that the before Flare-ECMEs are in average faster than the after Flare-ECMEs. The results show also both before and after Flare-ECMEs are wider than other CMEs. Besides it was found that the before Flare-ECMEs are in average faster than the after Flare-ECMEs, while the after Flare-ECMEs are in average more massive than before Flare – ECMEs. Finally it was found that both after and before Flare-ECMEs has negative mean acceleration.

ARTICLE HISTORY

Received 27 October 2020
Revised 7 December 2020
Accepted 26 December 2020

KEYWORDS

Solar Cycle- Solar Flares-
Coronal Mass Ejections

1. Introduction

Solar flares and coronal mass ejections, CMEs, are two important phenomena of the solar activity. The solar flare has visibly tense energy of any part of the release output in the low corona. It observed as a sudden intensity improvement in electromagnetic spectrum. CMEs are considered as magnetized plasma ejected from the solar corona that they considered as the core cause of geomagnetic storms (Youssef et al. 2013). Previous studies of CMEs recommended that there are two types of CMEs; CMEs associated with solar flares and CMEs which are not associated with flares. Mahrous et al. (2009) studied the relation between the solar flares and CMEs during solar cycle 23. They found a good linear positive relation between the CME energy and the X-ray flare. Youssef (2012) studied the CMEs and their associated solar flares during the period from 1996 to 2010. He found that the majority of the selected CME-Flare associated events ejected from the sun after the onset of their associated flares. This result withstands the idea that the flares produce CMEs as recommended by Dryer M (1996), not the idea that the flares are consequences of CMEs as proposed by Hundhausen (1999). Also (Youssef et al. 2013) examined the Post Flare-CME associated events by setting temporal and spatial condition. They found a practical relation between the CME speed and the flux of its associated solar flare. Aranio et al., (2011) have examined the relation of 826 CME-Flare associated events during the period from 1996 to 2006. They found a good correlation between the mass of the CMEs and the flux of their associated solar flares. Mawad. and Youssef. (2018) examined the properties of the selected CME-preflare associated events. They found

that the CME-preflare events are in average more massive and faster than all other CMEs during the same period. Also Mawad and Adel-Sattar (2020) studied the CMEs associated with gamma-ray bursts solar flares. They established that the CME initial speeds of the CME- γ -preflare associated events are meanly lower than solar wind mean speed and have the value 351 km/s, while non-associated CME has a mean value of 322 km/s.

In the present paper, we propose an investigation of some properties of ECMEs associated with solar flares which are observed during the period 1996–2006 to understand the properties of these more energetic CMEs.

2. Data bases and filtration

The used data in this study was obtained from the observations of X-ray flares and CMEs detected by GOES Satellite and the Large Angle and Spectrometric Coronagraph on board the Solar and Heliospheric Observatory SOHO/LASCO catalog. During the period from 1996 to 2006 GOES detected more than 20,000 solar flare events, where LASCO recorded about 12,000 CMEs. The spatial and time-based conditions were used to select the CME-Flare related events. Also solar wind flow speed data is obtained from coordinate Data Analysis Web CDAweb during the same period.

2.1. Time-based condition

We initially regulate the time gap to select CMEs ejected from the solar corona within \pm (1 h) from the onset time of their associated flares.

2.2. Spatial condition

Toward smear spatial condition, CMEs ejected from the solar corona need to be near the sites of their related flares on the solar surface, so the next condition essentially well be achieved:

$|\Psi_{\text{CME}} - \Psi_{\text{Flare}}| < \emptyset$ (Youssef, 2013), where Ψ_{CME} and Ψ_{Flare} are the position angle of the CME and solar flare on the solar disk respectively. \emptyset is the CME angular width.

3. Results and discussion

3.1. CME location on the solar disc

After the application of the above criteria, we obtained 253 energetic CMEs related to solar flares ((kinetic energy $\geq 1E + 30$ ergs) events of the total CMEs. Then we separated these 253 energetic CME-Flare events into two groups according to their time of detection, 132 Before Flare-ECME events (CMEs detected before solar flares onset) and 121 After Flare-ECME events (CMEs detected after flares). By using the same conditions criteria, Mahrous et al. (2009) found 224 CME-Flare related events during the solar cycle 23. Figure 1 shows Histogram of flare latitude and longitude of both before and after Flare-ECMEs. From this figure, we noticed that both before and after Flare-ECMEs are in average solar disc events

ejected from regions near the center of the solar disc. (Their latitudes and longitudes are $< \pm 30^\circ$).

3.2. CME angular width

The CME angular width is measured as the position angle size in the plane of sky. The average value of the CME width observed by SOHO is 47° (Yashiro et al. 2004). The normal CME width detected by Skylab and Solwind are 42° and 43° respectively which are in good agreement with LASCO result. While the mean CME width obtained from figure 2. for both before and after Flare-ECMEs are 90 and 100 degrees respectively. The present results for the average CME width are greater than the previous studies because of the selection of the energetic CMEs, where the most energetic CMEs have more wide CME width. Furthermore figure 3 illustrates that the after Flare-ECMEs have a number of halo CMEs more than the before Flare-ECMEs.

3.3. CME's speed

Youssef et al. (2013) found that the mean CME linear speed of the post Flare-CME associated events was 880 km/s, while the non related CMEs to flares speed have an average speed about

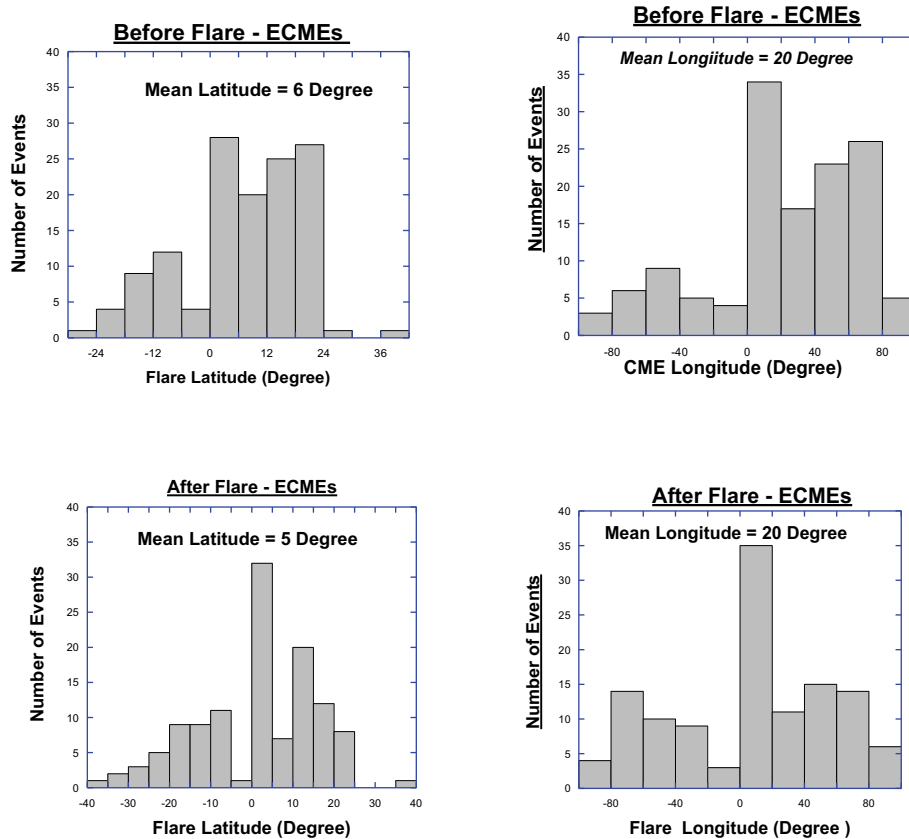


Figure 1. Histogram of flare latitude and longitude of both before and after flare-ECMEs.

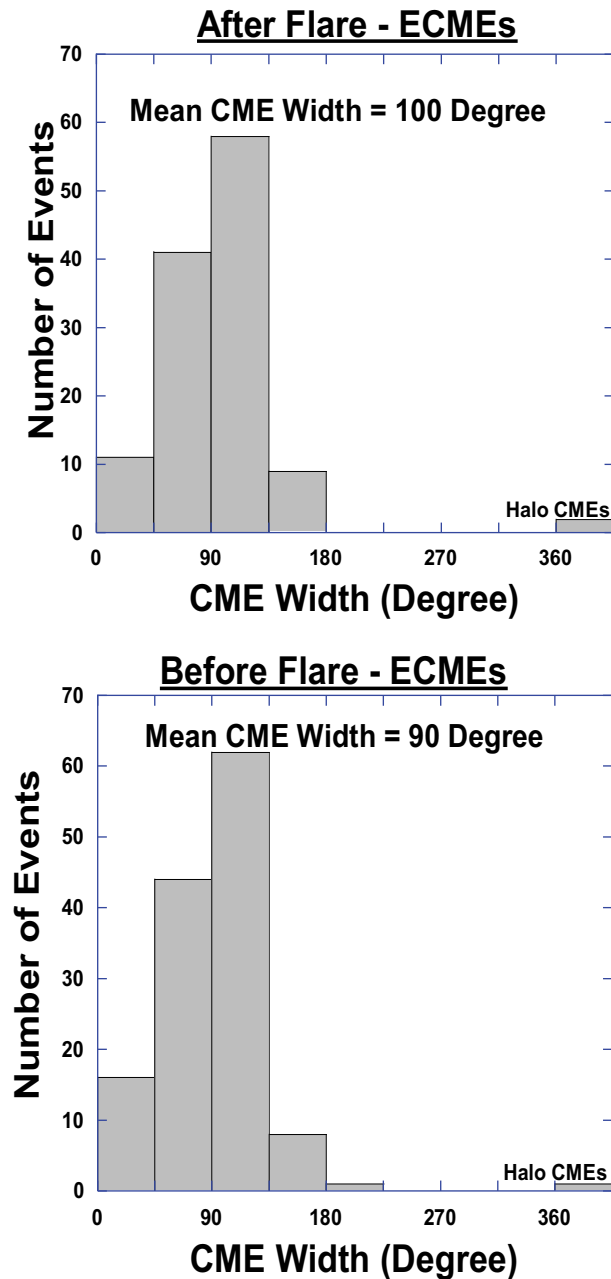


Figure 2. Histogram of CME width of both before and after Flare-ECMEs.

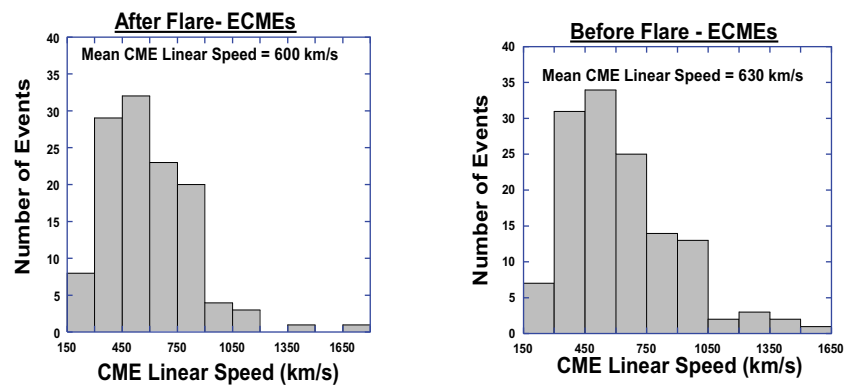


Figure 3. Histogram of CME linear speed of both before and after flare-ECMEs.

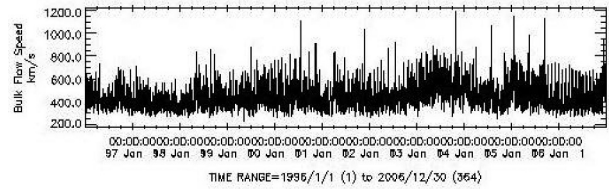


Figure 4. Time series of solar wind flow speed from January 1996 to December 2006.

400 km/s. While (Mawad, and Youssef, 2018) found that the CME linear speeds of CME-Preflare related events are crucially of the order of the solar wind speed. The results shown in figure 3, for the average CME linear speed of before Flare-ECMEs and after Flare-ECMEs are 630 km/s and 600 km/s respectively. The difference between my results and the results of previous studies may be attributed to difference of the period of each study. Figure 3 also shows that the before Flare-ECMEs are in average faster than the after Flare-ECMEs. Also if we compare the results mean CME linear speed in figure 3 to the mean solar wind speed as shown in figure 4 during the same period, we found that both after and before Flare-ECMEs are in average faster than the mean solar wind speed. This means that both CMEs normally drag the solar wind in the interplanetary space and lose some of their kinetic energies. Consequently both after and before Flare-CMEs must be decelerated and have in usual negative accelerations as cleared in the results of.

3.4. CME acceleration

Figure 5 shows that both after and before Flare-ECMEs has negative mean acceleration. This negative acceleration reflects how both after and before Flare-ECMEs interact with the solar wind in the

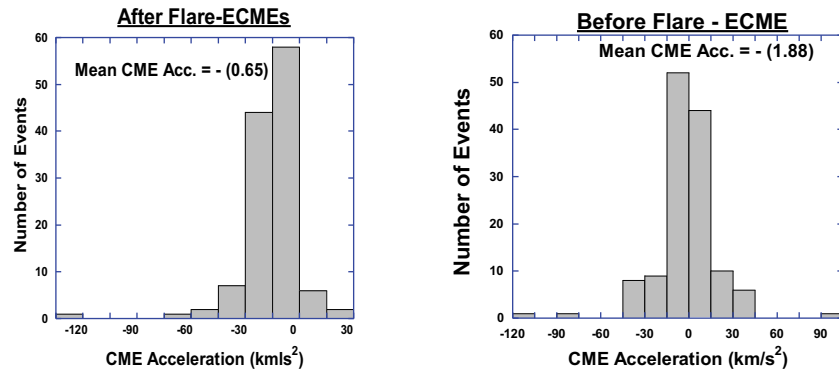


Figure 5. Histogram of CME acceleration of both before and after Flare-ECMEs.

interplanetary space, since Both CMEs are in average faster than the solar wind. This outcome is in arrangement with the result of Youssef et al. (2013) who found that the post flare-CME related events have average deceleration.

3.5. CME mass

The CME Mass is estimated by defining the number of electrons in the CME and the CME volume. By using radio observations both (Gopalswamy and Hanaoka 1998) and (Ramesh et al. 2003) evaluated the CME mass. While Gopalswamy et al. (1996) used x-ray remarks to estimate the mass of CMEs. These studies found that the mean values of the CME mass are in the order (10^{14} – 10^{15} g) which is generally lower than the average CME mass that we obtained of both before and after Flare-ECMEs as shown in figure 6. This is because the LASCO CME detections are based on the white-light mass observations not on radio nor x-ray observations. The average CME masses of after Flare-ECMEs and before Flare-ECMEs from figure 6 are $(3.705) \times 10^{15}$ g and $(3.537) \times 10^{15}$ g respectively, for the period from 1996 to 2010. The histograms in figure 6 obviously indicated that the after Flare-ECMEs are in normal more massive than before Flare-ECMEs.

Our results are in agreement with the results obtained by Vourlidis et al. (2011) and Shaltout et al. (2019).

3.6. CME mass-width relation

In figure 7 the logarithm of the CME mass is plotted as a function of the logarithm of CME width for both before and after Flare-ECMEs. R is the linear correlation coefficient which refers to the straight line relationship between two variables.

From figure 7 we can see that the linear correlation coefficient R of before Flare-ECMEs is greater than that for after Flare-ECMEs. R of before Flare-ECMEs is $= 0.58$ and for after Flare-ECMEs is $= 0.35$. Our results differ from the results obtained by Shaltout et al. (2019), where they found that the value of R for CME-Width relation of Flare-CME events during the solar cycle 24 for after and before Flare-ECMEs are $= 0.75$ and 0.85 , respectively. The difference in results might be attributed to the difference of the period of each study where our study covers the solar cycle 23 while Shaltout et al. (2019) focused their study during solar cycle 24. Or may be owing to the selection for only the energetic CMEs for the present study. The results in figure 7 also indicate that the mass of the before Flare-ECMEs are in average more correlated to their width than after Flare-ECMEs.

3.7. Flare properties of flare-ECMEs

The upper panel of figure (8a) demonstrates that both before and after Flare-ECMEs have in average the same

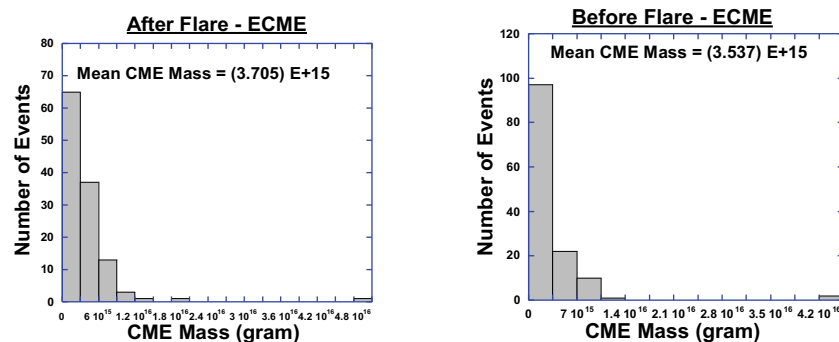


Figure 6. Histogram of CME mass of both before and after flare-ECMEs.

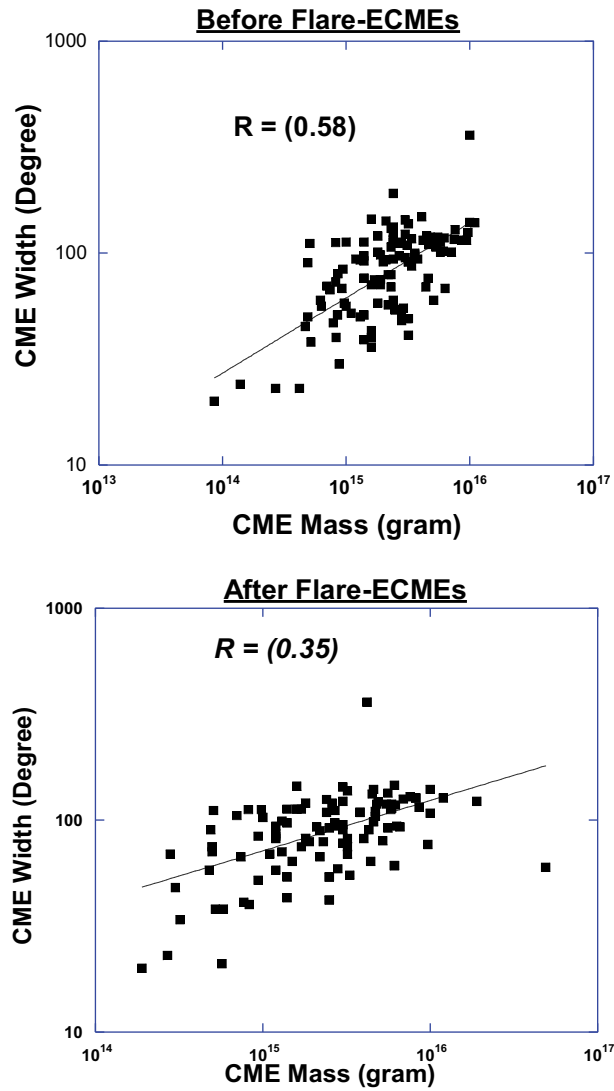


Figure 7. CME mass – width relation of both before and after flare -ECMEs.

flare intensity. While the lower panel of figure [figure \(8b\)](#) shows the histogram of flare class of both before and after Flare-ECMEs. It is easily to notice that the two CME class has the same behavior of the flare classification at the different levels of the solar cycle, where the number of events is smallest for flare B class, peaks for before C class and then declines through M and X class.

Also the lower panel of [figure 8\(b\)](#) shows that the distribution of flare class for both AF-ECMEs and BF-ECMEs has normal Gaussian distribution.

4. Conclusions

In the present paper, the study of the properties of energetic kinetic energy coronal mass ejections detected from 1996 to 2006 was carried out. During this period I selected 253 Flare-ECME associated events by using time-based and spatial circumstances. Then the separation of these 253 energetic CME-Flare events into two categories according to their time of detection was done

as Before Flare-ECME events and After Flare-ECME events. Finally we compared the physical properties of the two categories with each other and with the pervious studies. The main results of this study are as follows:

- (1) Both before and after Flare-ECMEs are in average solar disc events (ejected from regions near have longitudes and latitudes $< \pm 30^\circ$).
- (2) After Flare-ECMEs are in usual wider than before Flare-ECMEs.
- (3) Before Flare-ECMEs are in regular faster than the after Flare-ECMEs.
- (4) The after Flare-ECMEs are in normal more massive than before Flare-ECMEs.
- (5) Both after and before Flare-ECMEs has negative mean acceleration.
- (6) The histogram of flare class of both before and after Flare-ECMEs has the same behavior at the different levels of the solar cycle.
- (7) Both before and after Flare-ECMEs has in average the similar flare intensity.

Acknowledgements

The author thank N. Gopalswamy and his team for providing CMEs-related data to users through CDAW and for their contribution in making SOHO/LASCO catalog possible.

Disclosure statement

No potential conflict of interest was reported by the author.

References

- Aarnio AN, Stassun KG, Hughes WJ, McGregor SL. 2011. Solar flares and coronal mass ejections: a statistically determined flare flux - CME mass correlation. *Sol Phys.* 268(1):195–212. doi:10.1007/s11207-010-9672-7.
- Dryer M. 1996. *Solar Phys.* 169(2):421–429.
- Gopalswamy N, Hanaoka Y. 1998. Coronal dimming associated with a giant prominence eruption. *The Astrophysical Journal.* 498(2):L179. doi:10.1086/311330.
- Gopalswamy N, Kundu MR, Hanaoka Y, Enome S, Lemen JR, Akioka M. 1996. Yohkoh/SXT observations of a coronal mass ejection near the solar surface. *New Astron.* 1(3):207. doi:10.1016/S1384-1076(96)00016-4.
- Hundhausen A. 1999. Coronal mass ejections, in the many faces of the sun: a summary of the results from NASA's solar maximum mission (eds. Strong KT, Saba JLR, Haisch BM, Schmelz JT). New York: Springer; p. 143.
- Mahrous A, Shaltout M, Beheary MM, Mawad R, Youssef M. 2009. CME-flare association during the 23rd solar cycle. *Adv Space Res.* 43(7):1032–1035. ADS:2009AdSpR. doi:10.1016/j.asr.2009.01.028.
- Mawad R, Abdel-Sattar W. 2020. the characteristics of the coronal mass ejections preceding the associated X-ray and gamma ray bursts solar flares. *New Astron.* 74:101285. doi:10.1016/j.newast.2019.101285.
- Mawad. R, Youssef. M. 2018. A statistical study of CME-preflare associated events. *Adv Space Res.* 62 (2):417–425. doi:10.1016/j.asr.2018.04.040.

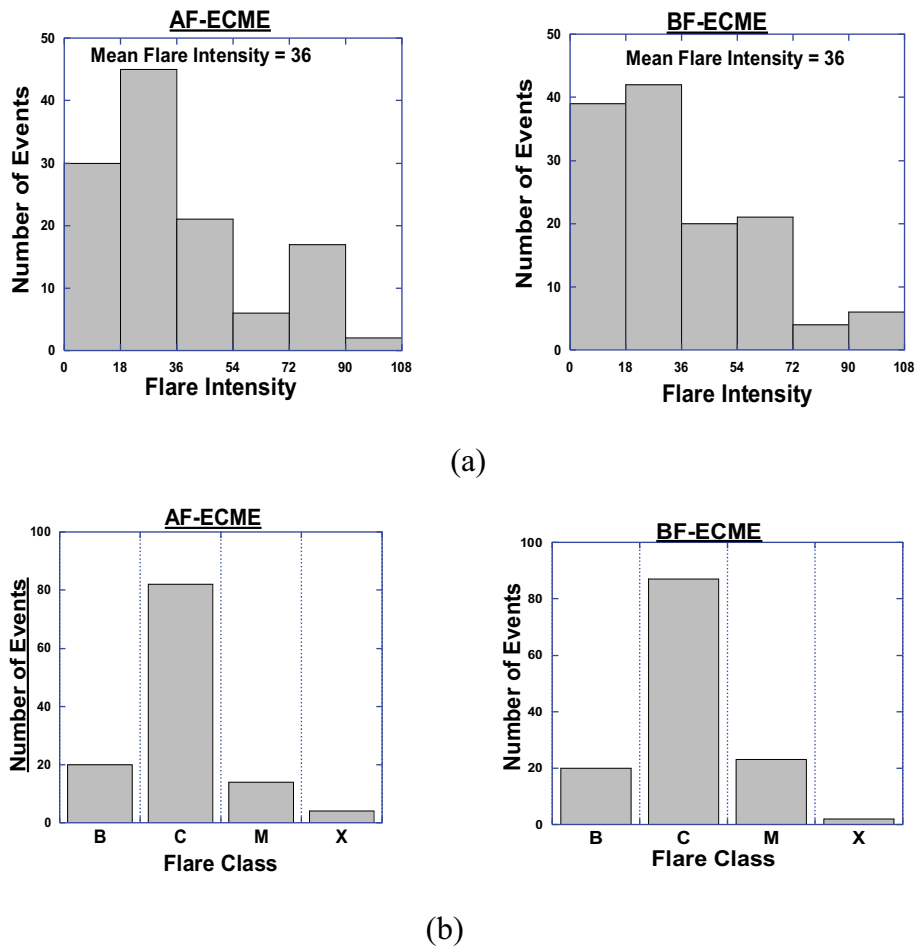


Figure 8. Histogram of flare intensity (a) and class (b) for both before and after flare-ECMEs.

Ramesh R, Kathiravan C, Sastry CV. 2003. Metric radio observations of the evolution of a “Halo” coronal mass ejection close to the sun. *The Astrophysical Journal*. 591 (2):L163. doi:10.1086/377162.

Shaltout AMK, Amin EA, Beheary MM, Hamid RH. 2019. A statistical study of CME-associated flare during the solar cycle 24. *Adv Space Res*. 63(7):2300–2311. doi:10.1016/j.asr.2018.12.022.

Vourlidas CA, Howard RA, Esfandiari E, Patsourakos S, Yashiro S, Michalek G. 2011. ERRATUM: “Comprehensive analysis of coronal mass ejection mass and energy properties over a full solar cycle” (2010, *ApJ*, 722, 1522). *The Astrophysical*

Journal. 730(1):59. doi:10.1088/0004-637X/730/1/59.

Yashiro S, Gopalswamy N, Michalek G, St. Cyr OC, Plunkett SP, Rich NB, Howard RA. 2004. A catalog of white light coronal mass ejections observed by the SOHO spacecraft. *J Geophys Res*. doi:10.1029/2003JA010282

Youssef M. 2012. On the relation between the CMEs and the solar flares. *NRIAG J Astron Geophys*. 1(2):172–178. doi:10.1016/j.nrjag.2012.12.014.

Youssef M, Mawad RM, Mosalam S. 2013. A statistical study of post-flare-associated CME events. *Adv Space Res*. 51 (7):1221–1229. ADS: 2013AdSpR.51.1221Y. doi:10.1016/j.asr.2012.10.007.